

# The Oxidation of Carbon Monoxide as an Integrated Part of the Coupled Alkane Oxidation Process: Gas-Phase Oxidation over Supported Metal-Complex Catalysts

E. G. Chepaikin<sup>a, \*</sup>, A. P. Bezruchenko<sup>a</sup>, G. N. Menchikova<sup>a</sup>, O. P. Tkachenko<sup>b</sup>,  
L. M. Kustov<sup>b, c</sup>, and A. V. Kulikov<sup>d</sup>

<sup>a</sup>Merzhanov Institute of Structural Macrokinetics and Materials Science, Russian Academy of Sciences,  
Chernogolovka, Moscow oblast, 142432 Russia

<sup>b</sup>Zelinskii Institute of Organic Chemistry, Russian Academy of Sciences, Moscow, 119991 Russia

<sup>c</sup>Department of Chemistry, Moscow State University, Moscow, 119991 Russia

<sup>d</sup>Institute of Problems of Chemical Physics, Russian Academy of Sciences,  
Chernogolovka, Moscow oblast 142432 Russia

\*e-mail: echep@ism.ac.ru

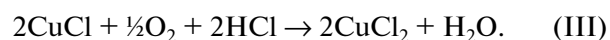
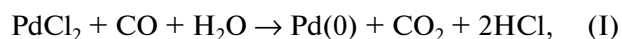
Received February 20, 2017

**Abstract**—Heterogeneous rhodium–copper chloride catalysts for gas-phase oxidation processes were prepared via the cold impregnation of  $\gamma$ -Al<sub>2</sub>O<sub>3</sub> with aqueous RhCl<sub>3</sub> and CuCl<sub>2</sub> solutions. Heptafluorobutyric or pentafluorobenzoic acids were additionally deposited onto these catalysts to simulate the action of homogeneous rhodium–copper chloride catalytic systems in the coupled alkane–carbon monoxide oxidation reaction. The catalysts were studied in the reactions of carbon monoxide oxidation and coupled propane–CO oxidation with dioxygen by diffuse reflectance IR Fourier transform spectroscopy (DRIFTS) and electron paramagnetic resonance (EPR). The obtained data indicate the probable transfer of electrons between rhodium and copper compounds.

**Keywords:** carbon monoxide, catalytic oxidation, rhodium chloride, copper chloride,  $\gamma$ -aluminum oxide, DRIFTS, EPR

**DOI:** 10.1134/S0023158418020039

Carbon monoxide oxidation is of great importance from both the theoretical viewpoint (the study of general problems on the mechanism of homogeneous catalytic reactions) and the practical viewpoint (detoxification of gas emissions, respiratory protection, and purification of hydrogen from CO). Homogeneous and heterogeneous palladium-containing catalysts are the most active in this reaction. The homogeneous catalysts [1–3] have been actively studied, usually as palladium metal complexes that are active in the presence of cocatalysts (reoxidants), such as salts of copper, iron, heteropoly acids, and quinones. CO oxidation in the presence of homogeneous systems can be simplistically schematized as follows:



Several other slightly modified schemes of this process have also been proposed. The intermediates that participate in this process are Pd(II) and, probably, Pd(I) carbonyls. It is implied that the reoxidation of

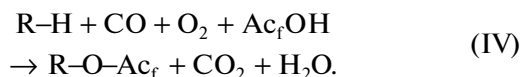
Pd(0) and Pd(I) by copper(II) occurs due to contact between them, most likely as a result of the formation of chloride bridges. The formation of such contacts in solutions is easy due to the high mobility of particles. Water is a component of the catalytic system. It is interesting that the presence of water is also necessary for the oxidation of CO on the heterogeneous Pd/ $\gamma$ -Al<sub>2</sub>O<sub>3</sub> catalyst. Surface hydroxyl groups of  $\gamma$ -Al<sub>2</sub>O<sub>3</sub> are incorporated into the catalytically active intermediate and further regenerated during the interaction of this catalyst with dioxygen [4].

The oxidation of carbon monoxide over the PdCl<sub>2</sub>–CuCl<sub>2</sub> catalytic system on different supports has been studied to create respiratory protection devices [5–10]. The reaction was conducted at low CO concentrations (<5 vol %) and room temperature, and the initial gas was saturated with water vapor. Since the adsorbability of  $\gamma$ -Al<sub>2</sub>O<sub>3</sub> with respect to water is high, it is possible that the catalytic reaction occurs in the water film on the  $\gamma$ -Al<sub>2</sub>O<sub>3</sub> surface [10].

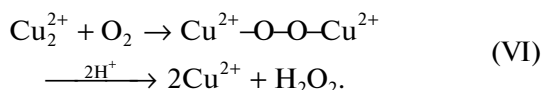
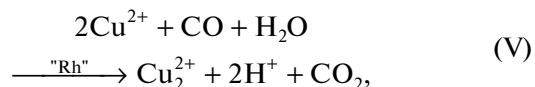
According to our preliminary data, the PdCl<sub>2</sub>–CuCl<sub>2</sub>/ $\gamma$ -Al<sub>2</sub>O<sub>3</sub> catalysts sustain self-heating (70–

80°C) at a CO concentration above 5 vol % due to the low efficiency of withdrawal of heat and lose activity due to the reduction of palladium to the metal state.

CO oxidation plays an essential part in such important reactions as the oxidation and oxidative carbonylation of alkanes. Carbon monoxide is a reducing agent (coreducer) of dioxygen. The direct partial oxidation of alkanes from natural and associated petroleum gases is considered as a promising method for the synthesis of key petrochemical products. The oxidation of alkanes over the traditional heterogeneous catalysts is characterized by a low selectivity due to the side deep oxidation process [11]. A much higher selectivity is demonstrated by the metal complex catalysts [12–14]. As a rule, they are more efficient in acidic media, in particular, in the presence of aqueous perfluorocarboxylic acids [12–20]. As shown by the studies of different oxygenases for the activation of dioxygen under mild conditions, it is necessary to complement the system with reducing agents [21], among which hydrogen and carbon monoxide are the most acceptable ones. Preference is given to CO, as CO<sub>2</sub> formed after its oxidation can easily be removed from a reactor. One of the most active catalysts for the coupled oxidation of alkanes and carbon monoxide is our rhodium–copper chloride system formed upon the dissolution of RhCl<sub>3</sub> · (H<sub>2</sub>O)<sub>3</sub> and copper compounds (CuO, Cu<sub>2</sub>O, and Cu(OAc)<sub>f</sub>) in an aqueous trifluoroacetic acid (Ac<sub>f</sub>OH) solution [18]:

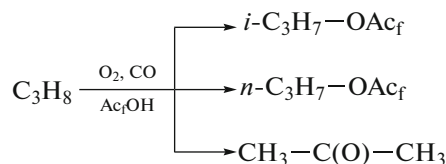


The role of CO consists of the conversion of dioxygen, which is inert under mild conditions, into active two-electron oxidants, such as hydrogen peroxide or its analogues over the catalytic system:



Some data [22] indicate that the reaction between Cu<sup>1+</sup> and dioxygen under certain conditions may lead to the accumulation of H<sub>2</sub>O<sub>2</sub> in an appreciable amount. We also considered some probable mechanisms of the action of this rhodium–copper chloride catalytic system with the participation of bridging heteronuclear intermediates that incorporate rhodium and copper and the activation of alkanes on peroxo

complexes [12–14, 19]. The homogeneous oxidation of propane generally occurs according to the scheme



The formation of small amounts of methyl- and ethyl-trifluoroacetates and formic, acetic, and propionic acids is also observed.

Since acidic media are aggressive, our work also included the preparation of heterogenized homogeneous catalysts for the gas-phase process to prevent the contact of these media with equipment. Such catalysts can be prepared via the deposition of homogeneous catalytic system solutions onto porous supports in solvents with high boiling temperatures (presumably, in the form of thin films). Similar catalysts in the form of an ionic liquid solution of a metal complex, which was immobilized on a support [23] or introduced into its pores [24], were studied earlier in hydroformylation reactions. The application prospects of catalysts of this type were considered in [25].

As can be judged from the results of studies on homogeneous catalytic systems [12–20], the coupled oxidation of CO and alkanes should be expected to occur at high CO concentrations (~10 vol %) and temperatures of no less than 80–90°C. The reduction of RhCl<sub>3</sub> with carbon monoxide into carbonyl complexes and the oxidation of carbon monoxide in the presence of rhodium carbonyls with participation of FeCl<sub>3</sub> and benzoquinones as stoichiometric oxidants have been studied in aqueous solutions [1].

The RhCl<sub>3</sub>–CuCl<sub>2</sub> catalytic system has almost not been studied in the considered reaction and the supported RhCl<sub>3</sub>–CuCl<sub>2</sub> composition has not been synthesized and studied at all by anyone until now. Nevertheless, it is much more stable at 80–90°C, but less active than the Pd-containing systems. Since the coupled oxidation of alkanes and carbon monoxide occurs at temperatures of no less than above-mentioned ones, the RhCl<sub>3</sub>–CuCl<sub>2</sub>/γ-Al<sub>2</sub>O<sub>3</sub> catalytic systems should be considered to be more promising than the Pd-containing catalysts. The gas-phase catalytic oxidation of carbon monoxide was studied on Rh/TiO<sub>2</sub> and Rh/Fe(OH)<sub>x</sub> catalysts and, for comparison, on Rh/Al<sub>2</sub>O<sub>3</sub> catalyst in [26, 27]. The activation of oxygen on Rh/Al<sub>2</sub>O<sub>3</sub> occurs at an increased temperature, while Rh/TiO<sub>2</sub> and Rh/Fe(OH)<sub>x</sub> are efficient at low temperatures. In the authors' opinion, this is due to the formation of heteronuclear structures such as Rh–O–O–Ti and Rh–O–O–Fe, which provide the possibility of successive competition between oxygen and carbon monoxide during their activation on a catalyst.

The objective of this work was to develop and study supported rhodium–copper chloride catalytic sys-

**Table 1.** Prepared catalysts and reference samples\*

Catalyst	Copper salt		Cu content, wt %	Acidic component	Acidic component content, wt %
	$\text{CuCl}_2 \cdot 2\text{H}_2\text{O}$	$\text{Cu}(\text{OAc})_2$ , wt %			
CT-1	+	—	3.5	—	—
CT-2	+	—	7.0	—	—
CT-3	+	3.04	6.54	—	—
CT-4	+	—	3.5	$\text{Pr}_f\text{COOH}$	5.7
CT-5	+	—	3.5	$\text{Ph}_f\text{COOH}$	5.0
CT-6	+	—	7.0	$\text{Pr}_f\text{COOH}$	5.0
CT-7	+	—	5.25	—	—
CT-8	+	—	5.25	$\text{Pr}_f\text{COOH}$	8.4
CT-9	+	—	3.5	—	—
CT-10	—	—	—	—	—
CT-11A	—	—	—	—	—
CT-12A	—	—	—	$\text{Pr}_f\text{COOH}$	7.5
CT-13A	+	—	3.5	—	—

\* Reference samples are CT-9 ( $\text{CuCl}_2/\gamma\text{-Al}_2\text{O}_3$ ), CT-10 ( $\text{RhCl}_3/\gamma\text{-Al}_2\text{O}_3$ ), CT-11A ( $\text{RhCl}_3/\gamma\text{-Al}_2\text{O}_3$ ), CT-12A ( $\text{RhCl}_3\text{—Pr}_f\text{COOH}/\gamma\text{-Al}_2\text{O}_3$  (7.5 wt %  $\text{Pr}_f\text{COOH}$ )), and CT-13A ( $\text{RhCl}_3\text{—CuCl}_2/\gamma\text{-Al}_2\text{O}_3$ ). The copper content in the copper-containing samples is 3.5 wt %. The rhodium content in all the samples except CT-9 is 1.5 wt %. The symbol A in the name of a sample means that it was treated with CO or a reaction vapor—gas mixture under catalytic reaction conditions.

tems, which would be predeterminedly active in homogeneous coupled alkane—CO oxidation reactions. The presence of copper salts promotes the activation of  $\text{O}_2$ . Their activity in the model carbon monoxide oxidation reaction was selected as a simple and convenient catalyst efficiency criterion. This criterion was used to determine the optimal conditions for the preparation of stable and active catalysts and to study the state of rhodium and copper in a catalyst and the possibility of their interaction on the surface of a support.

## MATERIALS AND METHODS

### Materials

$\text{RhCl}_3 \cdot (\text{H}_2\text{O})_n$  (34.5% Rh),  $\text{CuCl}_2 \cdot 2\text{H}_2\text{O}$  (chemically pure for analysis grade),  $\gamma\text{-Al}_2\text{O}_3$  (GOST (State Standard) 8136-85) in the form of 0.5–1-mm grains with a BET specific surface area of 205  $\text{m}^2/\text{g}$ , distilled water, and rectified acetone, methanol, propanol, *iso*-propanol, and *n*-butanol (all of chemically pure grade) were used in the experiments. Trifluoroacetic acid ( $\text{Ac}_f\text{OH}$ ) (Aldrich, 99%, extra-pure grade), heptafluorobutyric acid ( $\text{Pr}_f\text{COOH}$ ) (Aldrich, 99%, extra pure grade), and pentafluorobenzoic acid ( $\text{Ph}_f\text{COOH}$ ) (Aldrich, 99%, extra pure grade) were used without purification.

Copper trifluoroacetate  $\text{Cu}(\text{OAc}_f)_2$  was synthesized by dissolving CuO in  $\text{Ac}_f\text{OH}$  under boiling.

First, the hot solution was filtered;  $\text{Cu}(\text{OAc}_f)_2$  was then separated after cooling, dried in a vacuum, and stored in a exiccator.

CO (99.9%),  $\text{C}_3\text{H}_8$  (99.8%),  $\text{O}_2$  (99.9%), helium of grade A, electrolytic hydrogen, and purified atmospheric air were used as gaseous reagents.

### Preparation of Catalysts

To prepare CT-1–CT-3 catalysts (Table 1), a calculated amount of  $\text{RhCl}_3$  and  $\text{CuCl}_2$  was dissolved in distilled water (12 mL);  $\gamma\text{-Al}_2\text{O}_3$  (5 g) was then added and the mixture was allowed to stand for 12 h. Water was further distilled out on a rotary evaporator and the residue was dried at room temperature in air.

CT-4–CT-6 Catalysts were synthesized via the deposition of a calculated amount of  $\text{Pr}_f\text{COOH}$  or  $\text{Ph}_f\text{COOH}$  onto CT-1 from their solution in acetone. The latter was further distilled out on a rotary evaporator and the residue was dried in a vacuum at room temperature and allowed to stand in air. Reference catalysts CT-9 and CT-10 were synthesized by the same method as for CT-1.

### Catalytic Experiments

The experiments were performed on a flow-type setup (Fig. 1) at atmospheric pressure. The initial gas

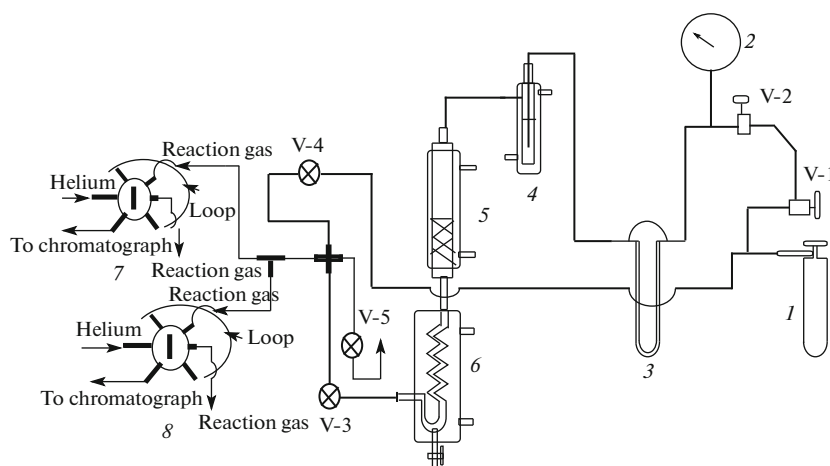


**Fig. 1.** Experimental setup: (1) bottle with a mixture of initial gases, (2) pressure gauge, (3) rheometer, (4) saturator for the saturation of gas with water vapor, (5) reactor with a temperature-controlled jacket, (6) condensing cooler, (7), (8) dosing valves for the introduction of samples into chromatograph columns; V-1 is the fine-control valve, V-2–V-5 are shutoff valves.

was prepared in steel bottle 1 by mixing the components, which were dosed with a reference pressure gauge and diluted to prevent the formation of explosive mixtures. In the coupled propane–CO oxidation experiments, the mixture was diluted with propane. The flow rate of the initial gas mixture was determined with precalibrated rheometer 3. The gas at the inlet into the reactor was saturated with water vapor, whose partial pressure was adjusted by changing the temperature in the jacket of steam bubbler 4. The steam bubbler height was 130 mm; the end of its inlet tube was equipped with a porous glass filtering plate to promote the formation of small bubbles and their saturation with water vapor. It turned out to be impossible to measure the moisture content with an IVTM-7 hygrometer due to flow pulsations despite that they were small. The pipeline from the bubbler to the reactor was carefully thermoinsulated to prevent the condensation of water. The amount of water entrapped in the condenser for 2–3 h was 0.75–0.85 of the calculated amount of the passed water vapor. Temperature in the jacket of reactor 5 (inner diameter, 9.5 m; height, 130 mm) was kept using a water thermostat. The gas at the outlet from the reactor was cooled in condenser 6 to separate water vapor. In the coupled propane–CO oxidation experiments, the trap was cooled to  $-40^{\circ}\text{C}$  to provide the entrapment of propane oxidation products. The cooled gas was passed to gas dosing valves 7, through which it was fed into a column with molecular sieves or valves 8 (into a Poparak Q column). Before the measurements, a vapor–gas mixture was passed through the reactor for 1 h to attain a steady-state regime. The composition of the outlet gas ( $\text{CO}$ ,  $\text{CO}_2$ ,  $\text{O}_2$ ) was then measured three times for 30–40 min together with its flow rate (with a foam rheometer).

The chromatographic data were used as a basis to determine the CO conversion and the catalyst activity ( $A$ ) as

$$A = \frac{WVC_{\text{CO}}^0 \alpha k}{10^4 \times 22.4m},$$

where  $W$  is the gas hourly space velocity (HSV) ( $\text{h}^{-1}$ ),  $V$  is the catalyst volume ( $\text{cm}^3$ ),  $C_{\text{CO}}^0$  is the CO content in the initial gas (%),  $\alpha$  is the CO conversion (%),  $k$  is the coefficient for the reduction of gas to normal conditions, and  $m$  is the amount of  $\text{RhCl}_3$  in a catalyst (mmol).

#### Analysis of Reaction Products

The gas and liquid phases were analyzed on a CrystallLux-4000M chromatograph (Meta-chrom, Russia) using NetChrom V2.1 software. The gas phase was analyzed at a column temperature of  $55^{\circ}\text{C}$  using helium as a carrier gas and a thermal conductivity detector, the analysis for  $\text{O}_2$ ,  $\text{N}_2$ ,  $\text{CH}_4$ ,  $\text{CO}$  was performed in a column, which was packed with 5-Å molecular sieves and had a length  $l = 3$  m and a diameter  $d = 3$  mm, at a grain size of 0.2–0.3 mm, and a carrier gas flow rate of 30 mL/min; the analysis for  $\text{CO}_2$  and propane was performed using Poparak Q as a packing with a grain size of 0.115–0.200 mm at  $l = 2$  m,  $d = 2.5$  mm, and a carrier gas flow rate of 20 mL/min. The liquid phase was analyzed using a flame ionization detector and an Agilent CP-Sil 5CB capillary column with  $l = 25$  m and  $d = 0.15$  mm at a temperature programmed from 40 to  $150^{\circ}\text{C}$  at a rate of 5 K/min, a He flow rate of 20 mL/min, an inlet column pressure of 1.3 atm, splitting the flow at a ratio of 1 : 70 at its rate of 0.287 mL/min.

The catalysts and reference samples were studied by diffuse reflectance IR Fourier transform spectros-

**Table 2.** Results of testing in the CO oxidation reaction for catalysts CT-1, CT-3, and CT-7\*

Experiment no.	Catalyst	$T$ , °C	Water vapor content, vol %	$W$ , h <sup>-1</sup>	$\alpha$ , %	$A$ , mol <sub>CO</sub> /(mol <sub>Rh</sub> h)
1	CT-1	50	2.8	251	69.0	9.7
2		60		249	80.0	11.2
3		70		251	83.7	11.9
4		80		280	92.4	14.8
5		90	2.8	351	88	17.4
6			19.8	780	87.6	38.6
7		50	2.8	250	68.1	9.6
8	CT-2	80	2.8	553	69.7	21.5
9		90	7.4	627	78.0	27.2
10	CT-3	80	2.8	277	23.6	3.3
11	CT-3 in 2 h			270	1.44	0.20
12	CT-7	90	7.4	1023	89.8	49.5

\* Catalyst weight, 2.1 g ( $V = 4.2 \text{ cm}^3$ );  $m_{\text{Rh}} = 0.3 \text{ mmol}$ . Gas composition (vol %): O<sub>2</sub>, 5.12; % CO, 9.67, helium, balance. Experiments 1–7 were performed on the same catalyst.

copy (DRIFT) on a NICOLET Protege 460 spectrometer (France) equipped with a diffuse reflectance attachment [28] developed in the Zelinskii Institute of Organic Chemistry of the Russian Academy of Sciences at room temperature in the region from 6000 to 400 cm<sup>-1</sup> at a step of 4 cm<sup>-1</sup>. To attain a satisfactory signal/noise ratio, 500 spectra were accumulated. CaF<sub>2</sub> was used as a standard. Before CO was fed into the ampoule with a catalyst it was evacuated to  $8 \times 10^{-2}$  Torr at room temperature for 5 min.

EPR spectra were recorded on a Radiopan SE/X 2544 spectrometer (Poland) at room temperature in ampoules with valves for the evacuation and feeding of gases. The second EPR spectrum integral ( $I$ ) normalized to three instrumental parameters (amplification coefficient, microwave power, and magnetic field modulation) was proportional to the number of paramagnetic sites in a catalyst. Carbon monoxide or air was fed into preevacuated ampoules until the atmospheric pressure was attained.

## RESULTS AND DISCUSSION

As shown earlier, homogeneous rhodium–copper chloride catalytic systems are efficient in an aqueous trifluoroacetic acid (Ac<sub>3</sub>OH) medium [12–14]. However, Ac<sub>3</sub>OH is not a suitable component for a heterogenized system due to its low boiling temperature (72.2°C). For this reason, heptafluorobutyric acid (melting temperature, 17.5°C; boiling temperature, 120°C) and pentafluorobenzoic acid (melting temperature, 100–102°C; boiling temperature, 220°C) were selected as acidic components. The most prom-

ising support (at least, for Pd-catalysts) is  $\gamma\text{-Al}_2\text{O}_3$  [4–8], which we also used. The composition of the catalysts and reference samples we prepared is given in Table 1. CT-1–CT-3 catalysts were compared with CT-4–CT-6 and CT-8 containing perfluorocarboxylic acids. In this case, we made the assumption that  $\gamma\text{-Al}_2\text{O}_3$  has the rather high acidity required for the oxidation of alkanes.

Catalyst testing results are given in Tables 2 and 3. From Table 2 it follows that CT-1 and CT-2 catalysts exhibit high activity ( $A$ ) and stability within a temperature range of 70–90°C, where (by analogy with the action of homogeneous catalysts) the coupled oxidation of propane and carbon monoxide can occur. The CT-3 catalyst containing copper partially in the form of Cu(OAc)<sub>2</sub> (see Table 1) proved to have low activity and was unstable (Table 2, experiments 10 and 11). The activity grows with an increase in the partial water-vapor pressure (experiments 5 and 6) and the copper content (experiments 4, 8 and 6, 9). Experiments 1 and 7 indicate the stability of the catalysts. The CT-7 catalyst was slightly more active than CT-2, probably due to its larger specific surface area. The use of copper in the form of CuCl<sub>2</sub> at a content of ~5% is optimal.

From Table 3 it follows that the introduction of perfluorocarboxylic acids slightly decreases the activity of catalysts. Nevertheless, the CT-4 basic catalyst still remains rather active (Table 3, experiments 1–4). It is noteworthy that CT-5, which contains the high boiling temperature Ph<sub>3</sub>COOH acid (boiling temperature 220°C) is also active. An increase in the copper content from 3.5 to 7.0 wt % improves the activity

**Table 3.** The results of testing in the CO oxidation reaction for catalysts CT-4, CT-5, and CT-6\*

Experiment no.	Catalyst	$T, ^\circ\text{C}$	Water vapor content, vol %	$W, \text{h}^{-1}$	$\alpha, \%$	$A, \text{mol}_{\text{CO}}/(\text{mol}_{\text{Rh}} \text{h})$
1	CT-4	70	3.0	231	70.4	8.5
2		70	7.4	360	49.0	10
3		80		490	56.8	14.0
4		90		542	47.4	17.5
5	CT-5	80	7.4	280	50.5	7.0
6		90		280	68.5	10.0
7	CT-6	80	9.4	425	60.0	11.5
8		90		434	76.3	14.4
					100	21.2**
9	CT-8***	90	9.6	633	19.5	15.7

\* Catalyst weight, 2.1 g ( $V = 4 \text{ cm}^3$ );  $m_{\text{Rh}} = 0.3 \text{ mmol}$ . Gas composition in experiments 1–6 and 9 (vol %):  $\text{O}_2$ , 5.20; CO, 9.10; helium, balance; gas composition in experiments 7 and 8 (vol %):  $\text{O}_2$ , 7.40; CO, 8.00; helium, balance.

\*\* The catalyst changed its color from beige to light yellow by 20 min after the beginning of experiment and its activity increased.

\*\*\* CT-8 weight, 1.06 g.

(experiments 3, 7 and 4, 8), and an increase in the  $\text{Pr}_f\text{COOH}$  content from 5.0 to 8.4%, on the contrary, slightly decreases it (experiments 4 and 9). Hence, perfluorocarboxylic acids introduced at 5–8 wt % slightly decrease the activity of catalysts, but increase their acidity as required for the coupled oxidation of alkanes and carbon monoxide. In experiment 8 (Table 3), this unexpectedly increased to  $A = 21.2 \text{ mol}_{\text{CO}}/(\text{mol}_{\text{Rh}} \text{h})$  in 20 min after a steady-state regime with an activity of  $14.4 \text{ mol}_{\text{CO}}/(\text{mol}_{\text{Rh}} \text{h})$  was attained and the catalyst changed its color from beige to light-yellow. It seems that the CT-6 catalyst may exist in at least two redox forms with different activities.

Attempts were made to perform the coupled oxidation of propane and carbon monoxide under the conditions specified in Tables 2 and 3 at 80 and  $90^\circ\text{C}$  (helium was replaced by propane); only traces of organic oxygenates were revealed among the reaction products. We also tried to use a catalyst containing 1.5 wt % Rh, 5 wt % Cu, and 8.5 wt %  $\text{Pr}_f\text{COOH}$  on  $\gamma\text{-Al}_2\text{O}_3$  pretreated with a 0.5 M sulfuric acid solution; however, the attempt was unsuccessful as well. The inactivity of these catalysts in the propane oxidation reaction may be explained by the fact that we did not manage to completely simulate the conditions for the homogeneous variant of this reaction (see, e.g., [20]).

#### Diffuse Reflectance IR Fourier Transform Spectroscopy

The eight different catalysts and reference samples that were studied were

(1)  $\text{RhCl}_3\text{--CuCl}_2/\gamma\text{-Al}_2\text{O}_3$  (1.5 wt % Rh, 3.5 wt % Cu) (CT-1);

(2)  $\text{RhCl}_3\text{--CuCl}_2\text{--Pr}_f\text{COOH}/\gamma\text{-Al}_2\text{O}_3$  (1.5 wt % Rh, 3.5 wt % Cu, 5.7 wt %  $\text{Pr}_f\text{COOH}$ ) (CT-4);

(3) CT-4A: catalyst CT-4 that was pretreated with CO and stored in a CO atmosphere;

(4)  $\text{CuCl}_2/\gamma\text{-Al}_2\text{O}_3$  (3.5 wt % Cu) (CT-9);

(5)  $\text{RhCl}_3/\gamma\text{-Al}_2\text{O}_3$  (1.5 wt % Rh) (CT-10);

(6)  $\text{RhCl}_3/\gamma\text{-Al}_2\text{O}_3$  (1.5 wt % Rh) (CT-11A);

(7)  $\text{RhCl}_3\text{--Pr}_f\text{COOH}/\gamma\text{-Al}_2\text{O}_3$  (1.5 wt % Rh, 7.5 wt %  $\text{Pr}_f\text{COOH}$ ) (CT-12A); and

(8)  $\text{RhCl}_3\text{--CuCl}_2/\gamma\text{-Al}_2\text{O}_3$  (1.5 wt % Rh, 3.5 wt % Cu) (CT-13A).

The assignment of spectral bands was accomplished with consideration for the literature data [29–32]. The panoramic spectra of catalysts and reference samples are shown in Fig. 2. As can be seen, the spectra of freshly prepared catalysts and reference samples do not differ from the spectrum of  $\gamma\text{-Al}_2\text{O}_3$  except CT-4A. The initial spectrum recorded for this catalyst in an air atmosphere contains three bands at 2079, 2023, and  $1804 \text{ cm}^{-1}$ . The first two of these belong to the anti-symmetric and symmetric vibrations of dicarbonyl  $\text{Rh}^+(\text{CO})_2$ . The band at  $1804 \text{ cm}^{-1}$  lies in the region of the absorption bands of bridging carbonyl groups [32] and could be assigned to the vibrations of such a group in the rhodium complex or the heteronuclear Rh–Cu compound. To determine the origin of this band, CT-11A reference samples (without Cu), CT-12A (without Cu, but with  $\text{Pr}_f\text{COOH}$ ) and CT-13A were prepared. Their spectra do not contain this band (Fig. 2). It follows that the band at  $1804 \text{ cm}^{-1}$  is not associated with the formation of the rhodium complex with a bridging carbonyl group or its heteronuclear analogue. This

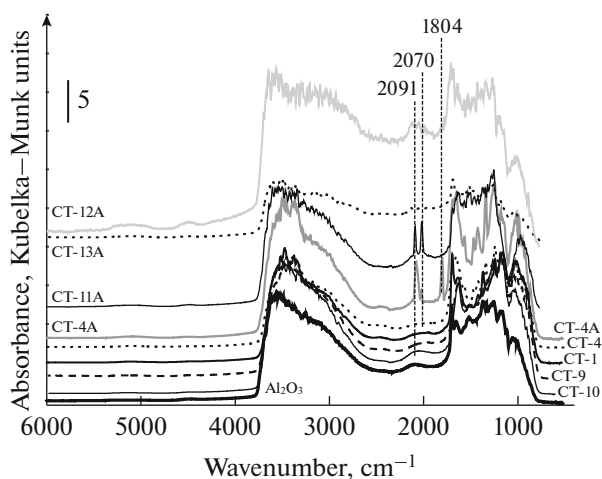


**Fig. 2.** Broad-range DRIFT spectra of the catalysts and reference samples.

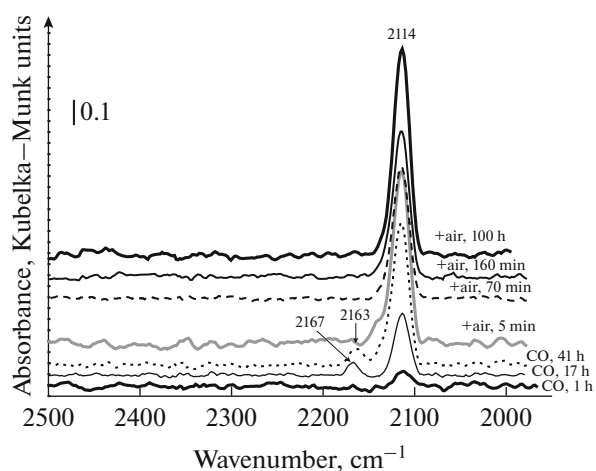


**Fig. 3.** DRIFT spectra of carbon monoxide and a CO + air mixture on the CT-9 catalyst.

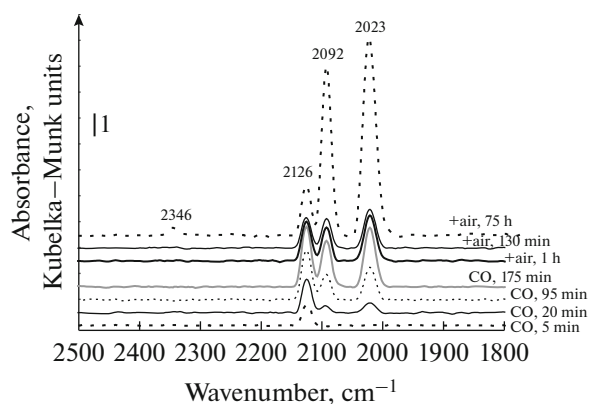


**Fig. 4.** DRIFT spectra of carbon monoxide and a CO + air mixture on the CT-10 catalyst.

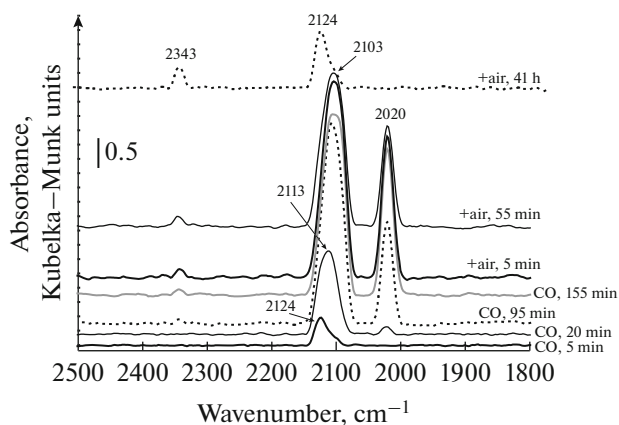


**Fig. 5.** DRIFT spectra of carbon monoxide and a CO + air mixture on the CT-1 catalyst.

band seems to be due to the presence of carbonate structures. The spectrum of the CT-9 catalyst exposed to a CO atmosphere (20–30 Torr) is characterized by the occurrence of the  $\text{Cu}^+(\text{CO})$  band at  $2114\text{ cm}^{-1}$ , which persists even 100 h after air was fed in (Fig. 3). At the initial stage of interaction between CT-9 and CO, the spectrum contains the  $\text{Cu}^{2+}(\text{CO})$  band at  $2167\text{ cm}^{-1}$ . The band of carbonyl complexes occurs in the spectrum of catalyst CT-10 under the same conditions as soon as in 5 min ( $\text{Rh}^{3+}(\text{CO})$  band at  $2126\text{ cm}^{-1}$  in Fig. 4). Bands at  $2092\text{ cm}^{-1}$  (antisymmetric  $\text{Rh}^+(\text{CO})_2$  vibrations) and  $2023\text{ cm}^{-1}$  (symmetric  $\text{Rh}^+(\text{CO})_2$  vibrations) then occur, and their intensity increases with time. In 175 h, the cell was filled with extra air to the atmospheric pressure, and the intensity of the bands at  $2092$  and  $2023\text{ cm}^{-1}$  had additionally increased in 75 h after this was accomplished. Hence, the formation of dicarbonyl  $\text{Rh}^+(\text{CO})_2$  continued even

in the presence of air. In this case, the spectrum also contains the  $\text{Rh}^{3+}(\text{CO})$  band. The reduction of  $\text{Rh}^{3+}(\text{CO})$  to  $\text{Rh}^+(\text{CO})_2$  leads to the occurrence of the adsorbed  $\text{CO}_2$  band ( $2345\text{ cm}^{-1}$ ).

Hence, air-stable carbonyl complexes of low-valence Rh and Cu ions are formed on the surface of CT-9 and CT-10. Both samples do not exhibit any catalytic activity in the CO oxidation reaction.

The interaction between CO and catalyst CT-1 first lead to the occurrence of the  $\text{Rh}^{3+}(\text{CO})$  band at  $2124\text{ cm}^{-1}$  (Fig. 5). The band at  $2020\text{ cm}^{-1}$  (symmetric  $\text{Rh}^+(\text{CO})_2$  vibrations) and the broadened band at  $2113\text{ cm}^{-1}$ , which is a superposition of bands from antisymmetric  $\text{Rh}^+(\text{CO})_2$  vibrations and  $\text{Cu}^+(\text{CO})$  vibrations, occur later on. The intensity of the bands at  $2020$  and  $2103\text{ cm}^{-1}$  increased with time. These bands disappeared in 41 h after air was fed in, thereupon the

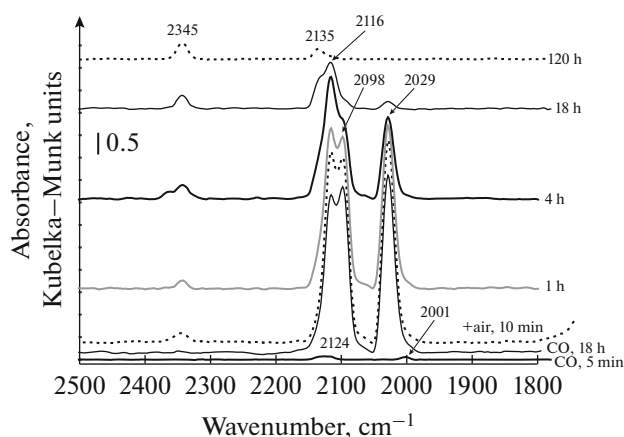


Fig. 6. DRIFT spectra of carbon monoxide and a CO + air mixture on the CT-4 catalyst.

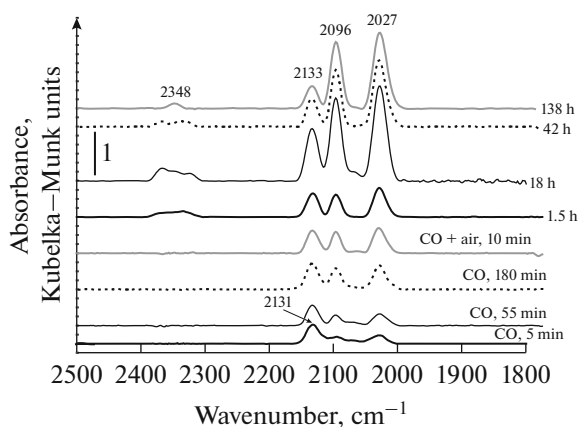


Fig. 7. DRIFT spectra of carbon monoxide and a CO + air mixture on the CT-12A catalyst.

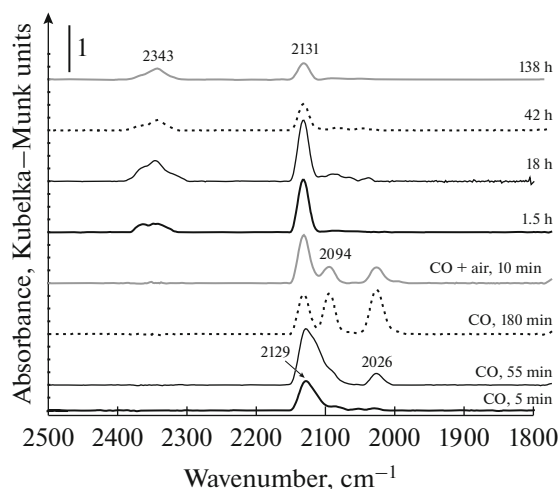


Fig. 8. DRIFT spectra of carbon monoxide and a CO + air mixture on the CT-13A catalyst.

$\text{Rh}^{3+}(\text{CO})$  band at  $2124\text{ cm}^{-1}$  with a shoulder at  $\sim 2114\text{ cm}^{-1}$  occurred probably due to the presence of  $\text{Cu}^+(\text{CO})$ . This indicates that reduced catalyst CT-1 is efficiently oxidized with air in contrast to CT-9 and CT-10.

The band assigned to a superposition of bands from antisymmetric  $\text{Rh}^+(\text{CO})_2$  and  $\text{Cu}^+(\text{CO})$  vibrations is shifted from  $2113$  to  $2103\text{ cm}^{-1}$  with time. It is likely that this shift is caused by the formation of heteronuclear carbonyl  $\text{Rh}^+$  and  $\text{Cu}^+$  complexes linked with each other by chloride, hydroxide, or oxide bridges. No alternative explanation seems possible for the configuration of the discussed spectra and the fact that the CO oxidation reaction is catalyzed.

The behavior of the CT-4 catalyst, which contained heptafluorobutyric acid in addition to  $\text{RhCl}_3$  and  $\text{CuCl}_2$ , is also interesting.  $\text{Pr}_f\text{COOH}$  was introduced as a high boiling temperature solvent and a strong acid, which is a necessary component of this catalytic system. The interaction with carbon monoxide leads to the occurrence of the band of symmetric  $\text{Rh}^+(\text{CO})_2$  vibrations at  $2029\text{ cm}^{-1}$ , i.e., it is shifted at  $6\text{ cm}^{-1}$  in comparison with the spectrum of the CT-1 catalyst (Fig. 6). Moreover, a partial resolution between the bands of antisymmetric  $\text{Rh}^+(\text{CO})_2$  and  $\text{Cu}^+-\text{CO}$  vibrations ( $2098$  and  $2116\text{ cm}^{-1}$ , respectively) is observed. The band at  $2345\text{ cm}^{-1}$  ( $\text{CO}_2$ ) occurs after air is fed in, while the other three bands persist for 4 h and then disappear. Only the band at  $2135\text{ cm}^{-1}$  ( $\text{Rh}^{3+}-\text{CO}$ ) remains in the spectrum in 120 h. Let us note that  $\text{Rh}^+(\text{CO})_2$  is more quickly oxidized than  $\text{Cu}^+(\text{CO})$ . According to the spectral data, the behavior of CT-4A almost does not differ from the behavior of CT-4.

Using a standard method, the CT-12A and CT-13A catalysts were also studied. The absorption bands assigned to carbonyl groups in the spectra of these catalysts are better resolved than in the spectra of CT-1, CT-4, and CT-10 (Figs. 7 and 8). This is likely to be due to the presence of  $\text{Pr}_f\text{COOH}$ . It is important to note that the spectrum of CT-13A does not contain the  $\text{Cu}^+-\text{CO}$  band at  $2114\text{ cm}^{-1}$ .

According to the X-ray diffraction data [8],  $\gamma\text{-Al}_2\text{O}_3$  supported copper exists in the form of paratacamite  $\text{Cu}_2\text{Cl}(\text{OH})_3$ , as was also confirmed by our X-ray diffraction data for the CT-1 catalyst ( $\text{RhCl}_3\text{-CuCl}_2/\gamma\text{-Al}_2\text{O}_3$ ). No rhodium has been revealed in the CT-1 and CT-10 catalysts; this indicates that it is amorphous and probably finely dispersed.

#### EPR Study of the Catalysts

The EPR spectra of freshly prepared CT-9 catalyst and the same catalyst treated in a CO atmosphere coincide with each other in their intensity ( $I$ ) and the shape of the signal (Fig. 9). Hence,  $\text{Cu(II)}$  is not subjected to any appreciable reduction to  $\text{Cu}^+(\text{CO})$  or Cu

under these conditions. The spectrum of CT-2 with an initial molar ratio  $\text{CuCl}_2 : \text{RhCl}_3 = 7.5$  contains the signal with  $g = 2.10$  and an intensity  $I = 15900$  arb. units (Fig. 10). The signals in the spectra of the catalyst and individual  $\text{CuCl}_2 \cdot 2\text{H}_2\text{O}$  (Fig. 10) differ from each other in their shapes. This is likely to be due to the formation of paratacamite or copper compounds, whose structure is close to paratacamite, on the surface of  $\gamma\text{-Al}_2\text{O}_3$ . After treatment in a CO atmosphere, the intensity of this signal abruptly decreases to  $I = 480$  (3% of the initial level). Hence, at least 7  $\text{Cu}^{2+}$  ions subjected to the reduction with carbon monoxide by reaction (V) catalyzed by rhodium complexes are available for the interaction with one  $\text{Rh}^+(\text{CO})_2$  ion.

The copper compound with a paratacamite structure is unlikely to be able to migrate over the surface due to steric hindrance and probably due to its rather strong bonding with  $\gamma\text{-Al}_2\text{O}_3$ . The analysis of DRIFTS spectra shows that rhodium in the reduced catalysts generally exists in the form of  $\text{Rh}^+(\text{CO})_2$ ; therefore, the possibility of its migration exists, which provides the interaction with  $\text{Cu}^{2+}$  via the formation of chloride bridges. From the analysis of EPR spectra it follows that copper in the CT-9 catalyst is not reduced in a CO atmosphere. Carbonyl  $\text{Cu}^+(\text{CO})$  revealed in the DRIFTS spectra of the CT-1, CT-4, and CT-9 catalysts seems to be formed in very small amounts from a certain especially active compound of copper, which is present in the freshly prepared samples and disappears after the catalytic reaction (e.g., in catalyst CT-13A).

Almost all the copper exists in the catalyst in the form of Cu(I) after treatment in a CO atmosphere, is not bonded to a carbonyl ligand and, in contrast to  $\text{Cu}^+(\text{CO})$ , can easily be oxidized with air oxygen to Cu(II), which further oxidizes Rh(I) containing particles. Hence,  $\text{Cu}^+(\text{CO})$  does not participate in the catalytic oxidation of carbon monoxide.

#### Interaction between the Catalyst Components

One of the important issues in estimating the effect of the catalysts we prepared and catalysts similar to them is the interaction between rhodium (or palladium) and copper compounds on the surface of  $\gamma\text{-Al}_2\text{O}_3$ . This issue was also mentioned in [8], where no signs of such an interaction could be revealed in freshly prepared catalysts, even using a large variety of physical methods. Heteronuclear  $[(\text{PdCl}_2)_2\text{CuCl}_2(\text{DMFA})_4]_n$  was separated out and characterized by X-ray diffraction when performing the Wacker process in a dimethylformamide (DMFA) medium, and  $[(\text{PdCl}_2)_6(\text{CuO})_4(\text{HMFT})_4]_n$  with oxo groups serving as bridges between Pd and Cu was identified when hexamethylphosphotriamide (HMFT) was used as a solvent [33]. It is possible to hypothesize that the interaction between the components of freshly prepared catalysts containing Rh(III) or Pd(II) and

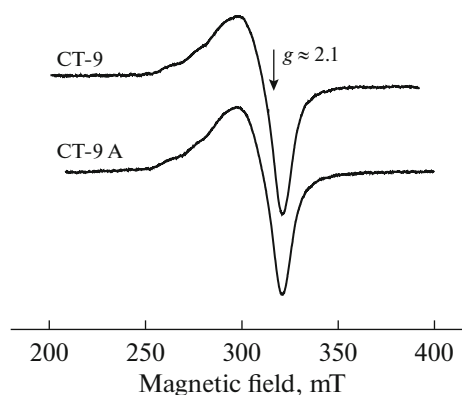


Fig. 9. EPR spectra of the CT-9 catalyst and the same catalyst treated with carbon monoxide (CT-9A) at room temperature.

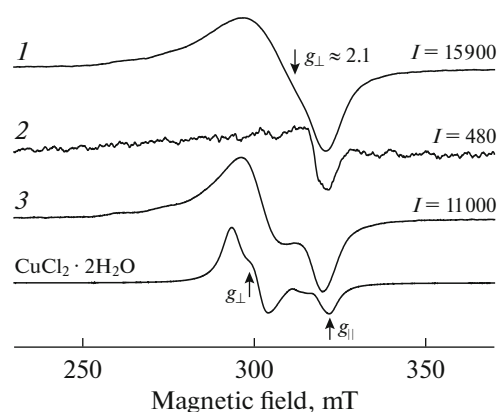


Fig. 10. EPR spectra recorded at room temperature for  $\text{CuCl}_2 \cdot 2\text{H}_2\text{O}$  and the CT-2 catalyst (1) without treatment and (2), (3) after treatment with (2) carbon monoxide and (3) air.

Cu(II) before their contact with CO is weak and is not exhibited in the spectra. Another factor may be associated with the peculiarities of catalyst preparation. As an example, the catalysts from the work [8] were evacuated to  $2 \times 10^{-8}$  Torr for 4 h for the removal of physically adsorbed water before recording their DRIFTS spectra. At the same time, the activity of catalysts appreciably increased after water vapor was added to the dry gas [7, 8]. Since our catalysts were subjected only to short-term evacuation before the addition of carbon monoxide, water and heptafluorobutyric acid (if used) might persist in a catalyst.

Hence, it has been demonstrated using DRIFTS and EPR that rhodium(I) carbonyl formed during the interaction of catalysts with carbon monoxide reduces Cu(II) to Cu(I). Here, there are up to seven Cu(II) ions available for the interaction with rhodium. This argues for the possibility of the migration of catalyst components or one of them (most probably, rhodium(I) carbonyl) over the solvent film on the support surface. Their migration may result in the formation of heteronuclear complexes with chloride, hydroxide, or

oxide bridges and the transfer of electrons between Rh(I) and Cu(II).

## CONCLUSIONS

In this work, heterogenized  $\gamma\text{-Al}_2\text{O}_3$  supported catalysts containing rhodium and copper compounds with and without perfluorocarboxylic acids were prepared for their testing in a coupled propane–carbon monoxide oxidation process. The catalysts were active and stable in the CO oxidation reaction at atmospheric pressure and a temperature up to 90°C; however, only traces of organic oxygenates were revealed when attempting to perform the coupled oxidation of propane and carbon monoxide under these conditions.

Using DRIFTS, it has been shown that carbonyl rhodium(I) and copper(I) complexes are formed in the prepared catalysts and reference samples. They are stable in air in the reference samples and subjected to oxidation in the catalysts. It is most likely that copper(I) carbonyl does not catalyze CO oxidation. As follows from the analysis of the EPR spectra, copper(II) in the reference sample is not reduced by carbon monoxide to any appreciable extent. Reduction takes place only in the presence of both rhodium and copper compounds. In this case, the intensity of the Cu(II) signal in the EPR spectrum decreases nearly to zero even at an initial atomic ratio Rh(III) : Cu(II) = 1 : 7.5. Hence, at least seven copper(II) ions are available for the interaction with rhodium.

## ACKNOWLEDGMENTS

The authors are grateful to D.Yu. Kovalev for performing the X-ray diffraction analysis. E.G. Chepaikin, A.P. Bezruchenko, and G.N. Menchikova are grateful to the Russian Foundation for Basic Research for financial support (project no. 17-03-00336). L.M. Kustov and O.P. Tkachenko are grateful to the Russian Scientific Foundation for financial support (grant no. 14-50-00126).

## REFERENCES

1. Sokol'skii, D.V. and Dorfman, Ya.A., *Kataliz ligandami v vodnykh rastvorakh (Catalysis by ligands in water solutions)*, Alma-Ata: Nauka, 1972.
2. Rakitskaya, T.L. and Paina, V.Ya., *Kinet. Katal.*, 1990, vol. 31, no. 2, p. 1393.
3. Kuznetsova, L.I., Matveev, K.I., and Zhizhina, E.G., *Kinet. Katal.*, 1986, vol. 26, no. 5, p. 1029.
4. Kakhniashvili, G.N., Mishchenko, Yu.A., Dulin, D.A., Isaeva, E.G., and Gel'bshtein, A.I., *Kinet. Katal.*, 1985, vol. 26, no. 1, p. 134.
5. Park, E.D. and Lee, J.S., *J. Catal.*, 2000, no. 1, p. 5.
6. Shen, Y., Lu, G., Guo, Y., and Gong, X., *Catal. Today*, 2011, vol. 175, p. 558.
7. Kotareva, I.A., Oshanina, I.V., Odintsov, K.Yu., Bruk, L.G., and Temkin, O.N., *Kinet. Katal.*, 2008, vol. 49, no. 1, p. 22.
8. Titov, D.N., Ustyugov, A.V., Tkachenko, O.P., Kustov, L.M., Zubavichus, Ya.V., Veligzhanin, A.A., Sadovskaya, N.V., Oshanina, I.V., Bruk, L.G., and Temkin, O.N., *Kinet. Catal.*, 2012, vol. 53, no. 2, p. 262.
9. Golodov, V.A., Sokolsky, D.V., and Noskova, N.F., *J. Mol. Catal.*, 1977, nos. 1–3, p. 51.
10. Lee, J.S. and Park, E.D., *Top. Catal.*, 2002, vol. 18, nos. 1–2, p. 67.
11. Arutyunov, V.S. and Krylov, O.V., *Okislitel'nye prevrashcheniya metana (Oxidative transformations of methane)*, Moscow: Nauka, 1998.
12. Chepaikin, E.G., *Usp. Khim.*, 2011, vol. 80, no. 4, p. 384.
13. Chepaikin, E.G., *J. Mol. Catal. A: Chem.*, 2014, vol. 385, p. 160.
14. Chepaikin, E.G. and Borshch, V.N., *J. Organomet. Chem.*, 2015, vol. 793, p. 78.
15. Sen, A., *Acc. Chem. Res.*, 1998, vol. 31, no. 9, p. 550.
16. Lin, M., Hogan, T., and Sen, A., *J. Am. Chem. Soc.*, 1996, vol. 118, no. 19, p. 4574.
17. Chepaikin, E.G., Bezruchenko, A.P., Leshcheva, A.A., Boyko, G.N., Kuzmenkov, I.V., Grigoryan, E.H., and Shilov, A.E., *J. Mol. Catal. A: Chem.*, 2001, vol. 169, p. 89.
18. Chepaikin, E.G., Bezruchenko, A.P., and Leshcheva, A.A., *Kinet. Catal.*, 2002, vol. 43, no. 4, p. 507.
19. Chepaikin, E.G., Bezruchenko, A.P., Boiko, G.N., Gekhman, A.E., and Moiseev, I.I., *Kinet. Catal.*, 2006, vol. 47, no. 1, p. 12.
20. Chepaikin, E.G., Bezruchenko, A.P., Menchikova, G.N., and Gekhman, A.E., *J. Mol. Catal. A: Chem.*, 2017, vol. 426, p. 389.
21. Shilov, A.E., *Metal Complexes in Biomimetic Chemical Reactions*, Boca Raton: CRC Press, 1997.
22. Zuberbuhler, A., *Helv. Chim. Acta*, 1967, vol. 50, no. 2, p. 466.
23. Mehnert, C.P., *Chem. – Eur. J.*, 2005, vol. 11, p. 50.
24. Haumann, M., Dentler, K., Joni, J., Rissager, A., and Wassersheid, P., *Adv. Synth. Catal.*, 2007, vol. 349, p. 425.
25. Oliver-Bourbigou, H., Magna, L., and Morvan, D., *Appl. Catal., A*, 2010, vol. 373, p. 1.
26. Guan, H.L., Lin, J., Qiao, B.T., Yang, X.F., Li, L., Miao, S., Liu, J.Y., Wang, A.Q., Wang, X.D., and Zang, T., *Angew. Chem.*, 2016, vol. 55, p. 2820.
27. Guan, H.L., Lin, J., Li, L., Wang, X.D., and Zang, T., *Appl. Catal., B*, 2016, vol. 184, p. 299.
28. Kustov, L.M., *Top. Catal.*, 1995, vol. 4, p. 131.
29. Davydov, A.A. *Molecular Spectroscopy of Oxide Catalyst Surfaces*, Hoboken: John Wiley & Sons, Inc., 2003, p. 466.
30. Hadjiivanov, K.I. and Vayssilov, G.N., *Adv. Catal.*, 2002, vol. 47, p. 307.
31. Sheppard, N. and Nguyen, T.T. *Advances in Infrared and Raman Spectroscopy*, Eds. Clark, R.J.H., Heste, R.E., vol. 5, chapter 2, London: Heyden and Son, 1978.
32. Kubiak, C.P. and Eisenberg, R., *J. Am. Chem. Soc.*, 1980, vol. 102, p. 3637.
33. Hosokawa, T., Nomura, T., and Murahashi, S.-I., *J. Organomet. Chem.*, 1998, vol. 551, p. 387.

Translated by E. Glushachenkova